

# WP 2362 - “Improved AOD@440nm: Satellite data collection and validation”

## Validation report on spatio-temporal ground-based vs satellite comparisons

Document reference: AOD440\_WP2362\_report  
Document Issue: 3.0  
Document Issue date: 31/10/2023  
Document authors and affiliations: M. Valeri<sup>1</sup>, S. Casadio<sup>1</sup>, L. Manunza<sup>1</sup>  
(1) Serco Italia S.p.A.

### AMENDMENT RECORD SHEET

The Amendment Record Sheet below records the history and issue status of this document.

ISSUE	DATE	REASON
1.0	31/05/2022	First draft of the report
2.0	28/07/2022	Updated including results of the inter-comparison exercise against MODIS Deep Blue and S-5P+ AOD products. Version 1 - Deliverable of project phase 1
3.0	31/10/2023	Updated reviewing previous versions and including the results of the inter-comparison against MODIS DB AOD products on Dhaka (Bangladesh), Mexico City (Mexico) and Beijing (China). Version 2 - Deliverable of project phase 2

## Contents

List of Acronyms .....	3
Reference Documents .....	3
2 Introduction .....	5
2 AOD products.....	5
2.1 AERONET AOD products.....	6
2.2 MODIS MAIAC AOD products.....	6
2.3 MODIS Deep Blue AOD products .....	7
2.4 Sentinel-3 SYNERGY AOD products .....	7
2.5 S-5P+ INNOVATION AOD products.....	8
3 Discussion .....	8
3.1 Inter-comparison of AERONET AOD products against MODIS MAIAC AOD data .....	8
3.2 Inter-comparison of AERONET AOD products against MODIS DB AOD data .....	15
3.2.1 Extension of the inter-comparison against MODIS DB AOD data to other sites .....	19
3.3 Inter-comparison of AERONET AOD products against S-3 SYN AOD data .....	22
3.4 Inter-comparison of AERONET AOD products against S-5P+ AOD data.....	26
4 Conclusions.....	30

## List of Acronyms

<b>AE</b>	Angström Exponent
<b>AERONET</b>	Aerosol Robotic NETwork
<b>AOD</b>	Aerosol Optical Depth
<b>BAQUNIN</b>	Boundary-layer Air Quality-analysis Using Network of Instruments
<b>BRDF</b>	Bidirectional reflectance distribution function
<b>DB</b>	Deep Blue
<b>ESA</b>	European Space Agency
<b>GRASP</b>	Generalized Retrieval of Aerosol and Surface Properties
<b>MAIAC</b>	Multi-Angle Implementation of Atmospheric Correction
<b>MODIS</b>	Moderate Resolution Imaging Spectroradiometer
<b>OLCI</b>	Ocean and Land Color Instrument
<b>QA</b>	Quality Assurance
<b>S-3</b>	Sentinel-3
<b>S-5P</b>	Sentinel-5 Precursor
<b>SLSTR</b>	Sea and Land Surface Temperature Radiometer
<b>SSA</b>	Single Scattering Albedo
<b>SZA</b>	Solar Zenith Angle

## Reference Documents

- [RD-1] Deliverable [D-2] from WP 2360: “Improved surface-based aerosol retrievals using NO<sub>2</sub> correction”, AODimprovements\_report.pdf, Panagiotis Ioannis Raptis, 2022
- [RD-2] Iannarelli, A. M., Di Bernardino, A., Casadio, S., Bassani, C., Cacciani, M., Campanelli, M., Casasanta, G., Cadau, E., Diémoz, H., Mevi, G., Siani, A. M., Cardaci, M., Dehn, A., & Goryl, P. (2022). The Boundary Layer Air Quality-Analysis Using Network of Instruments (BAQUNIN) Supersite for Atmospheric Research and Satellite Validation over Rome Area, Bulletin of the American Meteorological Society, 103(2), E599-E618. Retrieved May 16,

2022, from <https://journals.ametsoc.org/view/journals/bams/103/2/BAMS-D-21-0099.1.xml>

- [RD-3] Lyapustin, A., Wang, Y., Korkin, S., and Huang, D.: MODIS Collection 6 MAIAC algorithm, *Atmos. Meas. Tech.*, 11, 5741–5765, <https://doi.org/10.5194/amt-11-5741-2018>, 2018.
- [RD-4] Hsu, N. C., Jeong, M.-J., Bettenhausen, C., Sayer, A. M., Hansell, R., Seftor, C. S., Huang, J., and Tsay, S.-C.: Enhanced Deep Blue aerosol retrieval algorithm: The second generation, *J. Geophys. Res.-Atmos.*, 118, 9296–9315, <https://doi.org/10.1002/jgrd.50712>, 2013.
- [RD-5] Dubovik, O., Herman, M., Holdak, A., Lapyonok, T., Tanré, D., Deuzé, J. L., Ducos, F., Sinyuk, A., and Lopatin, A.: Statistically optimized inversion algorithm for enhanced retrieval of aerosol properties from spectral multi-angle polarimetric satellite observations, *Atmos. Meas. Tech.*, 4, 975–1018, <https://doi.org/10.5194/amt-4-975-2011>, 2011.
- [RD-6] Dubovik, O., T. Lapyonok, P. Litvinov, et al.: GRASP: a versatile algorithm for characterizing the atmosphere, *SPIE: Newsroom*, Published Online: September 19, 2014. doi:10.1117/2.1201408.005558
- [RD-7] Drosoglou, T., Raptis, I.-P., Valeri, M., Casadio, S., Barnaba, F., Herreras-Giralda, M., Lopatin, A., Dubovik, O., Brizzi, G., Niro, F., Campanelli, M., and Kazadzis, S.: Evaluating the effects of columnar NO<sub>2</sub> on the accuracy of aerosol optical properties retrievals, *Atmos. Meas. Tech.*, 16, 2989–3014, <https://doi.org/10.5194/amt-16-2989-2023>, 2023.
- [RD-8] Papachristopoulou, K., Raptis, I.-P., Gkikas, A., Fountoulakis, I., Masoom, A., and Kazadzis, S.: Aerosol optical depth regime over megacities of the world, *Atmos. Chem. Phys.*, 22, 15703–15727, <https://doi.org/10.5194/acp-22-15703-2022>, 2022.
- [RD-9] Ichoku, C., Chu, D. A., Mattoo, S., Kaufman, Y. J., Remer, L. A., Tanré, D., Slutsker, I., and Holben, B. N.: A spatio-temporal approach for global validation and analysis of MODIS aerosol products, *Geophys. Res. Lett.*, 29(12), doi:10.1029/2001GL013206, 2002.
- [RD-10] Sogacheva, L., Denisselle, M., Kolmonen, P., Virtanen, T. H., North, P., Henocq, C., Scifoni, S., and Dransfeld, S.: Extended validation and evaluation of the OLCI–SLSTR SYNERGY aerosol product (SY\_2\_AOD) on Sentinel-3, *Atmos. Meas. Tech.*, 15, 5289–5322, <https://doi.org/10.5194/amt-15-5289-2022>, 2022.

## 2 Introduction

The aerosol optical depth (AOD) is probably the most comprehensive and used variable for assessing the aerosol load in the atmosphere. During the last decades, satellite and ground-based remote sensing observations have become widely used to monitor aerosols' spatial and temporal distributions on a global and local scale. Satellite instruments, such as Moderate Resolution Imaging Spectroradiometer (MODIS), monitor aerosols on a regional and global scale and provide long-term and continuous coverage. Observations from ground-based stations have higher measurement precision at low spatial reach. Such ground-based optical networks for aerosols monitoring, like AErosol RObotic NETwork (AERONET), use sun photometers or sun-sky radiometers. Unfortunately, the AOD retrieval from sun-photometric measurements is sensitive to the concentration of atmospheric gases such as nitrogen dioxide ( $\text{NO}_2$ ), particularly in spectral regions in which light absorption is significant. Currently, either satellite climatological  $\text{NO}_2$  datasets are used to estimate  $\text{NO}_2$ -related optical depth in the AOD retrievals, or  $\text{NO}_2$  is not considered at all in such calculations. However, due to inhomogeneous local emission patterns and photochemical destruction,  $\text{NO}_2$  is characterized by a relatively short lifetime and high spatial and temporal variations, especially in polluted areas, such as the area of Rome. For this reason, climatological values rarely represent the actual  $\text{NO}_2$  loading and spatial distribution in the atmosphere, introducing non-negligible errors in AOD retrievals in spectral regions with high absorption from  $\text{NO}_2$ . In this report, we assess the improvement of existing AOD and Ångström exponent (AE) datasets by applying a correction using synchronous and collocated measurements of total  $\text{NO}_2$  column with respect to reference satellite AOD products. All the details about the methodology adopted for the computation of the correction are reported in [RD-1]. The inter-comparison has been performed over two close (about 13 km) sites in Rome, Italy, namely the Rome La Sapienza University and ISAC-CNR in Rome Tor Vergata, characterized as urban and suburban sites, respectively. The existing AERONET AOD datasets and the “improved” ones have been compared against four satellite AOD products: the MODIS Terra and Aqua combined Multi-angle Implementation of Atmospheric Correction (MAIAC) AOD products, the MODIS Deep Blue (DB) AOD products, the Sentinel 3 SYNERGY AOD products retrieved exploiting co-registered Ocean and Land Color Instrument (OLCI) and Sea and Land Surface Temperature Radiometer (SLSTR) Level 1b radiances, and the AOD products retrieved using S-5P+/TROPOMI measurements and the Generalized Retrieval of Aerosol and Surface Properties (GRASP) approach.

## 2 AOD products

This section briefly introduces the ground-based and satellite AOD products used in the inter-comparison exercise. Regarding the ground-based information, we used the AERONET AOD data for Rome La Sapienza and Rome Tor Vergata sites. Concerning satellite AOD data used for evaluating AERONET AOD products and the corresponding quality, we performed the inter-comparison against several satellite datasets. We used the MAIAC and Deep Blue datasets that exploit the MODIS observation, the AOD products retrieved using S-5P/TROPOMI measurements and the GRASP approach, and the AOD products estimated by exploiting the synergies between SLSTR and OLCI onboard S3 satellites.

## 2.1 AERONET AOD products

AERONET is a ground-based sun and sky scanning radiometer network that measures aerosol optical properties worldwide. Aerosol optical and microphysical properties in the AERONET database include AOD, AE, refractive index, size distribution, single scattering albedo (SSA), absorption AOD, and asymmetry factor. Aerosol properties are derived from the direct and diffuse solar spectral radiance measured by CIMEL CE318 sun-photometers. In this exercise, we used Version 3 Level 1.5 AERONET AOD data (freely available at <https://aeronet.gsfc.nasa.gov/>). These data are cloud-cleared, and quality controls have been applied, but these data may still need to have final calibration applied. This data may change in Level 2.0, but they represent a good trade-off between quality and readiness, keeping in mind that our approach aims to perform a near-real-time correction on AERONET AOD products. We extracted all the AERONET AOD data at 440 nm for Rome La Sapienza and Rome Tor Vergata sites. The CIMEL at Rome La Sapienza is located on the roof of the Fermi Building at La Sapienza University (Latitude: 41.90169° North, Longitude: 12.51577° East, Elevation: 75.0 Meters), part of the BAQUNIN super-site (<https://www.baqunin.eu/>, [RD-2]). The CIMEL in Rome Tor Vergata is installed at the CNR Isac Rome Atmospheric obSservatory (CIRAS) at the CNR Research Area in Rome Tor Vergata. These two different AERONET sites in Rome are about 13 km distant.

As well as an assessment of the quality of the official AERONET AOD products for both sites in Rome, this inter-comparison aims to assess the “improvement” of existing AOD and AE datasets by applying a correction using synchronous and collocated Pandora NO<sub>2</sub> measurements. All the details about the methodology adopted for the computation of the correction are reported in [RD-1].

## 2.2 MODIS MAIAC AOD products

MODIS is a key instrument aboard the Terra and Aqua satellites. Terra MODIS (pass from north to south across the equator in the morning) and Aqua MODIS (pass south to north over the equator in the afternoon) are observing the entire Earth's surface every 1 to 2 days, acquiring data in 36 spectral bands ranging in wavelength from 0.4 μm to 14.4 μm, with a spatial resolution of 1 km at nadir (except for a few bands with higher spatial resolution).

The MCD19A2 Version 6 data product is a MODIS Terra and Aqua combined Multi-angle Implementation of Atmospheric Correction (MAIAC, <https://pdaac.usgs.gov/products/mcd19a2v006/>, [RD-3]) Land AOD gridded Level 2 product produced daily at 1 km pixel resolution. The MCD19A2 AOD data product contains the following Science Dataset (SDS) layers: blue band AOD at 0.47 μm, green band AOD at 0.55 μm, AOD uncertainty, fine mode fraction over water, column water vapour over land and clouds (in cm), smoke injection height (m above ground), AOD QA, AOD model at 1 km, cosine of solar zenith angle, cosine of view zenith angle, relative azimuth angle, scattering angle, and glint angle at 5 km.

As suggested in [RD-3], we considered as valid AOD products, the pixels where QA\_AOD = Best\_Quality which combines the best values of cloud and adjacency masks

- QA.CloudMask = Clear

- QA.AdjacencyMask ( $\pm 2$  pixel vicinity) = Clear

During the inter-comparison with AERONET products, we considered the valid MODIS MAIAC products within a grid of dimension of 1x1, 5x5 and 15x15 km centered at site location and over the 2017-2022 period. The agreement between the two datasets has been evaluated as a function of the grid dimension and of the temporal co-location criteria.

### 2.3 MODIS Deep Blue AOD products

MODIS Deep Blue (DB) [RD-4] algorithm was developed for aerosol retrieval on bright surfaces. The basic principle of DB algorithms is to utilize the pre-calculated land surface reflectance database in deep blue bands (0.412  $\mu\text{m}$ ), in which surface reflectance is relatively lower than those in longer bands.

For this exercise, we used the Collection 6.1 DB AOD products for both Aqua and Terra satellites. The spatial resolution of this product is 10 km. The inter-comparison was performed using MODIS DB AOD at 470 nm. For this reason, the AERONET AOD at 470 nm was computed using the AERONET AOD at 440 nm and AERONET Angstrom Exponent (AE\_440\_870). In this analysis, we tested different co-location criteria: we considered MODIS DB AOD products within an area of radius 1, 5 and 15 km around the AERONET site location and the AERONET AOD data with  $\Delta t_{\text{max}}$  between the MODIS satellite overpasses and AERONET observations of  $\pm 15$ ,  $\pm 30$  and  $\pm 60$  minutes. In order to guarantee the adequate quality of the data, we used MODIS DB data with  $qa_{\text{index}} \geq 2$ , which corresponds to good and very good products. To avoid possible effects caused by the presence of water surfaces, such as lakes, within the MODIS pixel, we have used only the MODIS DB pixel that does not contain water surfaces. The inter-comparison was performed in the 2017-2021 period.

### 2.4 Sentinel-3 SYNERGY AOD products

The S-3 SYN AOD products take benefit of the spectral and angular capabilities of the co-registration of OLCI and SLSTR L1b radiances over the same grid. All relevant L1b datasets are averaged on a super-pixel resolution defined at 4.5 km<sup>2</sup>. Note that only radiometry associated with clear-sky pixels is considered in this averaging. The aerosol characteristics are provided for both land and sea pixels. Over the land, the algorithm uses as inputs to the aerosol retrieval module both SLSTR views (nadir and oblique) and all channels (except S4, i.e., 1.37  $\mu\text{m}$ , dedicated to cloud detection) + one OLCI channel: Oa3, 442.5 nm. In addition to the retrieved aerosol parameters, S-3 SYN AOD products provide contextual parameters such as time, quality flags, solar and satellite angles, and geographical position. The processing of super-pixels to estimate aerosol properties is based on optimization by iterative numerical inversion, with the propagation of uncertainties. The full algorithm is described in the product ATBD (S3-L2-AOD-SYN-ATBD, v1.12). The inter-comparison was performed in the 2020-2022 period considering areas with radius of 10 km and 25 km centered on the sites' location. In particular, the 25 km spatial criteria follows the approach adopted in [RD-9] and [RD-10], where a surface of ca. 50 km x 50 km around each station is considered for the matchup identification.

## 2.5 S-5P+ INNOVATION AOD products

ESA S5P+Innovation AOD/BRDF project is focused on aerosol and surface reflectance characterization using capabilities of S-5P/TROPOMI measurements (<https://eo4society.esa.int/projects/sentinel-5p-innovation-aod-brdf/>). More specifically, the project's main objective is to have an integrated retrieval algorithm for characterizing aerosol load and type of the aerosol and BRDF products from S-5P TROPOMI using the Generalized Retrieval of Aerosol and Surface Properties (GRASP, <https://www.grasp-open.com>) approach. GRASP retrieval is implemented as a highly advanced statistically optimized fitting of all available observations. In addition, GRASP uses an innovative multi-pixel concept in which the fitting is realized simultaneously for a large group of “pixels”. This approach is useful for improving satellite retrievals where it allows benefitting from known a priori limitations on space and time variability of different surface and aerosol parameters.

For this exercise, we considered only S-5P/TROPOMI AOD products within a maximum distance of 5 and 15 km from the AERONET site (considering the center of the TROPOMI pixel). We also tested different temporal criteria: we considered AERONET AOD data with  $\Delta t_{\max}$  between AERONET observations and satellite overpass of  $\pm 15$ ,  $\pm 30$ , and  $\pm 60$  minutes. S-5P/TROPOMI AOD data are available only for 2019-2020. The data are available at [https://www.grasp-sas.com/projects/aod-brdf\\_sentinel-5p-innovation/](https://www.grasp-sas.com/projects/aod-brdf_sentinel-5p-innovation/) in the section “Data” (registration is needed). In order to guarantee the adequate quality of the data, we used only the S-5P/TROPOMI AOD products with  $qa_{\text{index}} \geq 2$ , that represent good and very good quality products.

## 3 Discussion

This section describes the methodology that we adopted and the results of the inter-comparison between AERONET, “improved” and not, AOD products at 440 nm and the different satellite borne AOD products.

### 3.1 Inter-comparison of AERONET AOD products against MODIS MAIAC AOD data

Since AERONET retrieval is performed at 440 nm and MODIS AOD is retrieved at 470 nm, we exploited the AERONET AE between 440 and 870 nm to derive AERONET AOD at 470 nm and we used the equation:

$$\tau_{470} = \tau_{440} \left( \frac{\lambda_{470}}{\lambda_{440}} \right)^{-\alpha}$$

where  $\tau_{470}$  is the AOD at 470 nm,  $\tau_{440}$  is the AOD at 440 nm,  $\alpha$  is the AE between 440 and 870 nm,  $\lambda_{440}$  is 440 nm, and  $\lambda_{470}$  is 470 nm. In the example reported in Fig. 1, we show co-located MODIS MAIAC and AERONET AOD products considering all the MODIS products in a 5 x 5 km grid centered on the AERONET sites and a  $\Delta t_{\max}$  between the MODIS satellite overpasses and AERONET observations of  $\pm 30$  minutes.



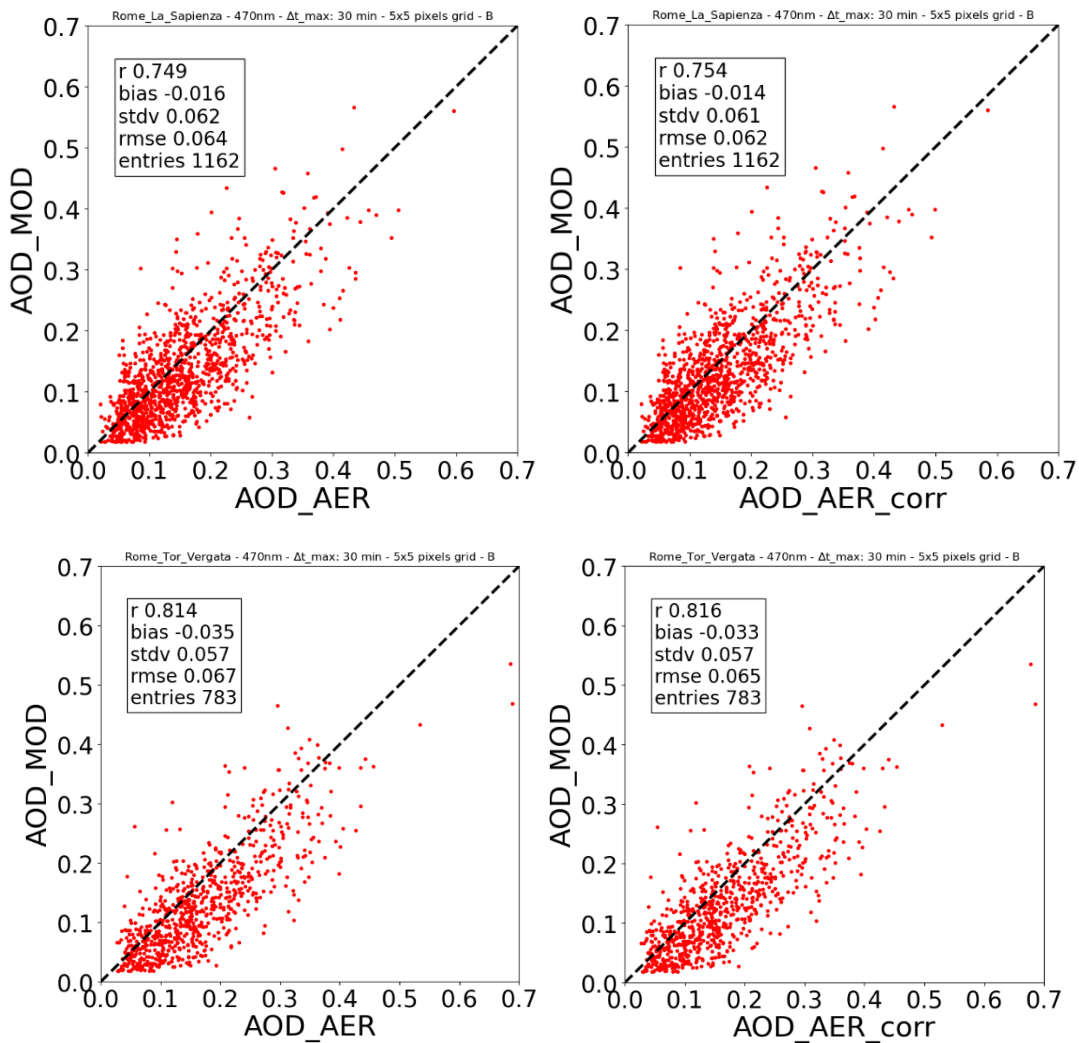


**Figure 1:** Inter-comparison of MODIS MAIAC and AERONET AOD (left column) and MODIS MAIAC and “improved” AERONET (right column) AOD at 470 nm for Rome La Sapienza (upper row) and Rome Tor Vergata (lower row) sites. The example reported here was performed considering 5x5 km grid centered at site location and  $\Delta t_{max}$  (time between MODIS MAIAC and AERONET observations) of  $\pm 30$  minutes. Both MODIS Aqua and Terra satellites are considered.

The correction introduces a slight improvement (0.002 on average) in the agreement between the two AOD products. Generally, we can observe that the differences between MODIS MAIAC and AERONET AOD products are larger (about 2 times) for the Rome Tor Vergata site with respect to the Rome La Sapienza site, even if the correlation between the two datasets is higher for this AERONET site. We evaluated the “improvement” at 470 nm, computed as the AERONET AOD (computed using AOD440\_AER and AE\_440\_870) minus the “improved” AERONET AOD (computed using corrected AOD440\_AER and corrected AE\_440\_870) as a function of the MODIS AOD at 470nm. We did not observe evident dependency of the correction by the AOD absolute value. Despite the “improvement” being on average

of the order of 0.002, in Fig. 2, we can better highlight as some “improvements” are of the order of 15/20%.

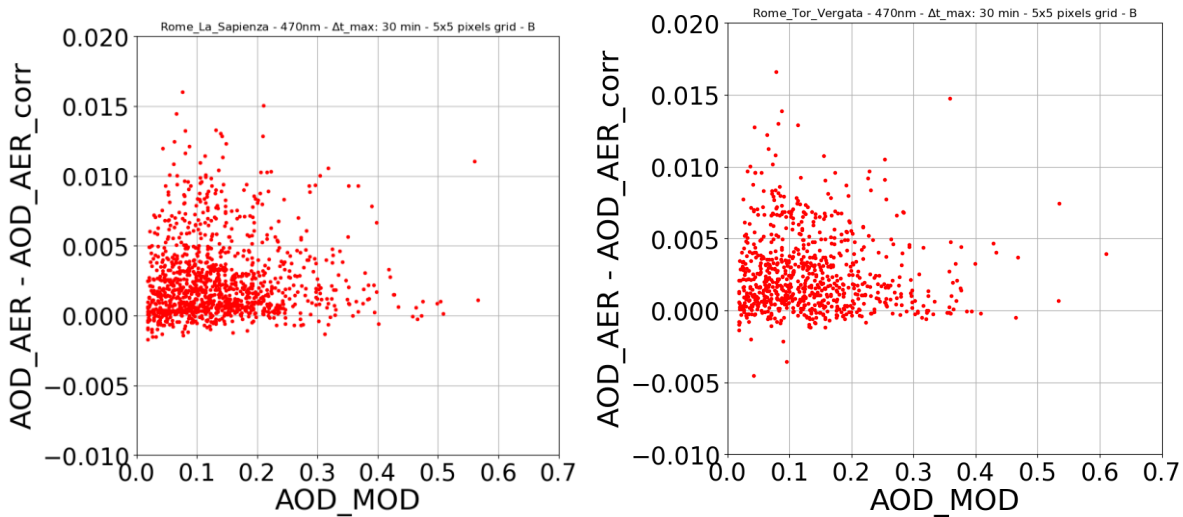


**Figure 2:** Analysis of the “improvement” computed as the AERONET AOD minus the “improved” AERONET AOD, as a function of MODIS MAIAC AOD at 470 nm for Rome La Sapienza (upper row) and Rome Tor Vergata (lower row) sites. The example reported here was performed considering 5x5 km grid centered at site location and  $\Delta t_{max}$  (time between MODIS MAIAC and AERONET observations) of  $\pm 30$  minutes. Both MODIS Aqua and Terra satellites are considered.

To better evaluate the possible dependency of the agreement between MODIS MAIAC and AERONET AOD products and the “improvement” from the period of the year, we computed the monthly averages of the different AOD datasets, the differences (MODIS MAIAC minus AERONET) and the “improvement” for both Rome La Sapienza and Rome Tor Vergata sites.

For both stations, we generally observed a lower agreement between AERONET and MODIS MAIAC AOD at 470 nm in the summer period and the best in autumn (crosses in the upper panel of each plot), where we observed even slightly positive bias (MODIS MAIAC > AERONET). The “improvement” is about 0.002 for both sites. Even if the “improvement” is extremely slight on average, it goes in the right direction to cope with the differences between AERONET and MODIS MAIAC AOD at 470 nm. Anyway, the analysis does not highlight explicit dependency of the correction by the month.

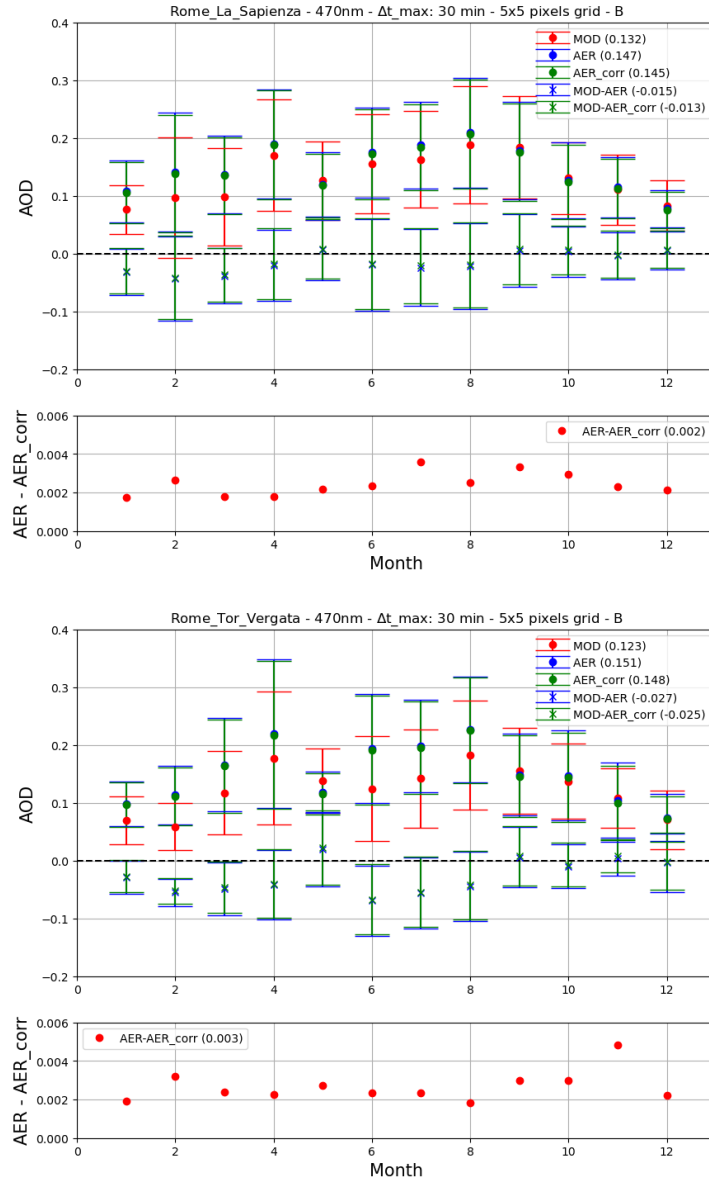


**Figure 3:** Analysis of the differences between MODIS MAIAC and AERONET AOD at 470 nm (upper panel of each plot) and of the “improvement” computed as the AERONET AOD minus the “improved” AERONET AOD, (lower panel of each plot) as a function of the month for Rome La Sapienza (upper plot) and Rome Tor Vergata (lower plot) sites. The example reported here was performed considering 5x5 km grid centered at site location and  $\Delta t_{max}$  (time between MODIS MAIAC and AERONET observations) of  $\pm 30$  minutes. Both MODIS Aqua and Terra satellites are considered.

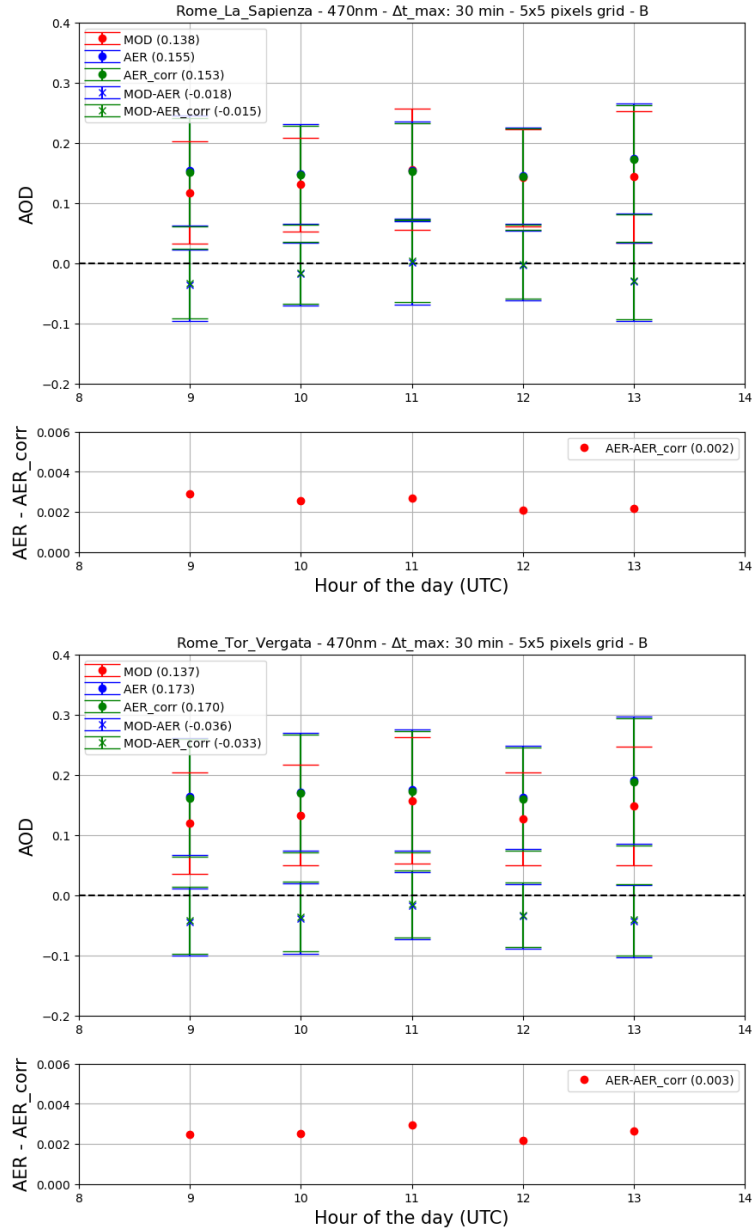


**Figure 4:** Analysis of the differences between MODIS MAIAC and AERONET AOD at 470nm (upper panel of each plot) and of the “improvement” computed as the AERONET AOD minus the “improved” AERONET AOD, (lower panel of each plot) as a function of the hour of the day for Rome La Sapienza (upper plot) and Rome Tor Vergata (lower plot) sites. The example reported here was performed considering 5x5 km grid centered at site location and  $\Delta t_{max}$  (time between MODIS MAIAC and AERONET observations) of  $\pm 30$  minutes. Both MODIS Aqua and Terra satellites are considered.

Following the same approach, we also analysed the possible dependency of the differences (MODIS MAIAC minus AERONET) and the “improvement” from the hour of the day, computing the averages of the different datasets as a function of the hour of the satellite overpasses for both Rome La Sapienza and Rome Tor Vergata sites. For both stations, we generally observed a better agreement between AERONET and MODIS MAIAC AOD at 470 nm at the central hour of the day (12 and 13 UTC), corresponding to the lowest SZA. The analysis does not highlight explicit dependency on the “improvement” by the hour of the day. The “improvement” is 0.002 for Rome La Sapienza and 0.003 for Rome Tor Vergata and it goes in the right direction.

				MOD 470nm vs AER 470nm			MOD 470nm vs improved AER 470nm		
Site	Grid	$\Delta t_{max}$ (minutes)	N	Bias (MOD-AER)	Std. Dev.	Corr	Bias (MOD-AER)	Std. Dev.	Corr
Rome La Sapienza	1x1	15	959	-0.021	0.063	0.715	-0.019	0.062	0.721
		30	979	-0.021	0.062	0.723	-0.018	0.062	0.728
		60	997	-0.02	0.062	0.723	-0.018	0.061	0.728
	5x5	15	1133	-0.017	0.062	0.742	-0.014	0.061	0.748
		30	1162	-0.016	0.062	0.749	-0.014	0.061	0.754
		60	1189	-0.015	0.062	0.745	-0.013	0.061	0.749
	15x15	15	1316	-0.017	0.061	0.785	-0.015	0.06	0.789
		30	1375	-0.016	0.061	0.792	-0.013	0.06	0.796
		60	1431	-0.014	0.062	0.784	-0.012	0.062	0.788
Rome Tor Vergata	1x1	15	663	-0.036	0.056	0.82	-0.033	0.055	0.823
		30	713	-0.035	0.057	0.812	-0.033	0.057	0.814
		60	761	-0.036	0.057	0.809	-0.033	0.056	0.811
	5x5	15	719	-0.035	0.056	0.818	-0.032	0.056	0.821
		30	783	-0.035	0.057	0.814	-0.033	0.057	0.816
		60	839	-0.034	0.057	0.807	-0.032	0.057	0.81
	15x15	15	816	-0.029	0.062	0.797	-0.026	0.062	0.8
		30	906	-0.028	0.065	0.779	-0.025	0.065	0.783
		60	986	-0.026	0.066	0.771	-0.023	0.065	0.775

**Table 1:** Results of the analysis of the differences of MODIS MAIAC (both Terra and Aqua) and AERONET AOD and MODIS MAIAC and “improved” AERONET AOD at 470 nm for Rome La Sapienza and Rome Tor Vergata sites. The differences, the standard deviations and the correlations are reported as a function of the different spatio-temporal criteria adopted in the analysis: 1x1, 5x5 and 15x15 km for the spatial criteria, and  $\pm 15$ ,  $\pm 30$  and  $\pm 60$  minutes for the temporal criteria.

The results shown until this point are computed considering a 5 x 5 km grid centered at the site location and  $\Delta t_{max}$ , the time between MODIS MAIAC and AERONET observations, of  $\pm 30$  minutes. Considering the distance between the two sites and the temporal variability of aerosol distribution, the co-location criteria mentioned above represent the most meaningful criteria from a physical point of view. Anyway,

as already introduced, we performed the same analysis even considering different criteria: 1 x 1 and 15 x 15 km for the spatial criteria (dimension of the grid centered on the AERONET site location) and  $\pm 15$  and  $\pm 60$  minutes for the temporal criteria. The results of the analysis are reported in Table 1. To improve the readability of the results, we also summarize in Fig. 5 the analysis of the difference between MODIS MAIAC and AERONET, original and “improved”, AOD at 470 nm as a function of the co-location criteria for both AERONET sites.

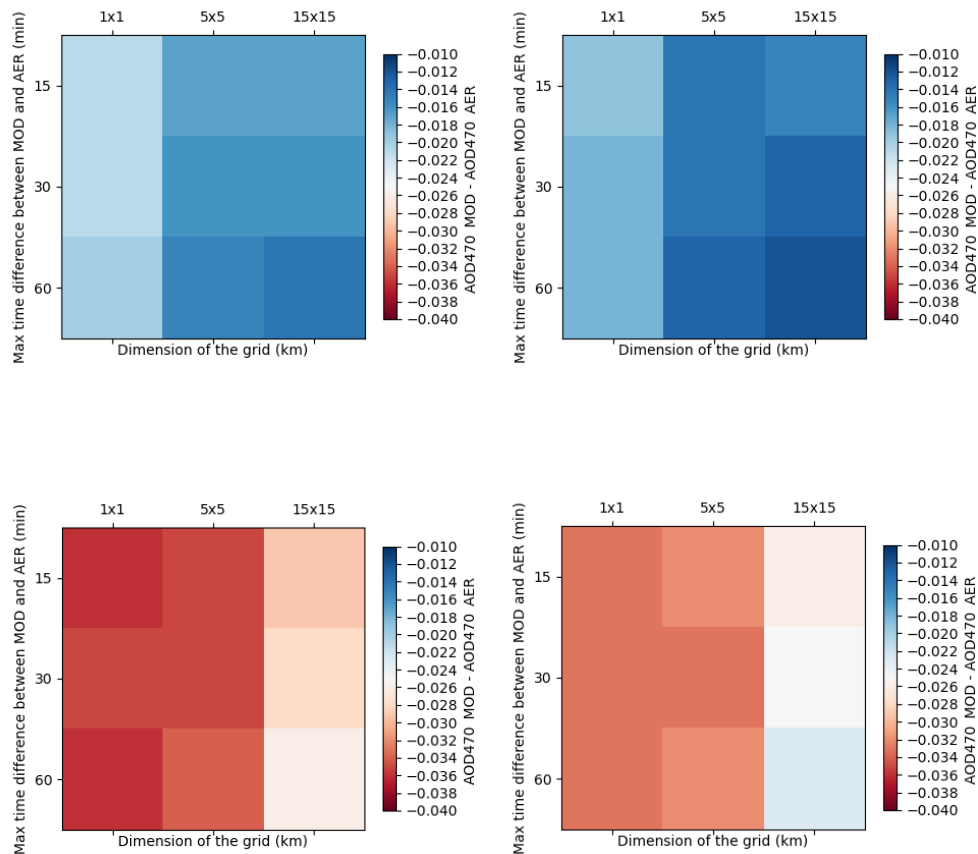


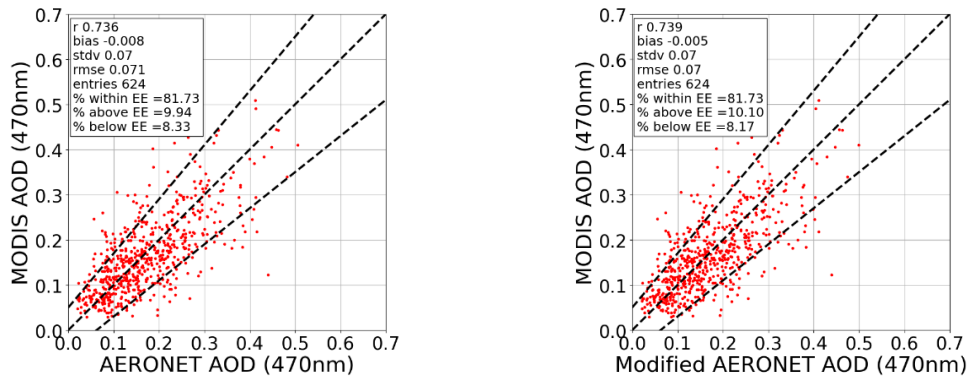
**Figure 5:** Analysis of the differences of MODIS MAIAC and AERONET AOD (left column) and MODIS MAIAC and “improved” AERONET (right column) AOD at 470nm for Rome La Sapienza (upper row) and Rome Tor Vergata (lower row) sites. The differences in each plot are reported as a function of the different spatio-temporal criteria adopted in the analysis: 1x1, 5x5 and 15x15 km for the spatial criteria, and  $\pm 15$ ,  $\pm 30$  and  $\pm 60$  minutes for the temporal criteria.

In Tab. 1 and Fig. 5, we can observe as the difference decreases as the area's dimension increases (true for both original and improved AERONET) for Rome Tor Vergata site because we also consider darker surfaces, where the retrieval algorithm works better. For the same reason, the standard deviation should increase as the area's dimension increases (not shown here). We also observed that considering the most relaxed co-location criteria, the standard deviation and correlation of the two sites are almost equal

because we are considering almost the same aerosol distribution or area. This is not true for the bias that considering the same criteria is about two times higher for the Rome Tor Vergata site. This last aspect is probably related to possible instrument issues or different parameters within the retrieval algorithm.

### 3.2 Inter-comparison of AERONET AOD products against MODIS DB AOD data

APL-SAP - 470nm -  $\Delta t_{max}$ :30min - 5x5 pixels grid - B APL-SAP - 470nm -  $\Delta t_{max}$ :30 - 5x5 pixels grid - B



CNR-ISAC - 470nm -  $\Delta t_{max}$ :30min - 5x5 pixels grid - B CNR-ISAC - 470nm -  $\Delta t_{max}$ :30 - 5x5 pixels grid - B

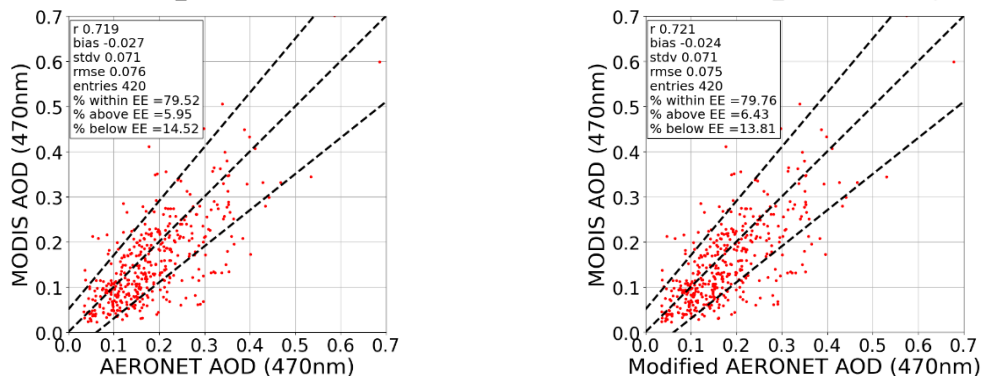


**Figure 6:** Inter-comparison of MODIS DB and AERONET AOD (left column) and MODIS DB and “Modified” AERONET (right column) AOD at 470nm for Rome La Sapienza (upper row) and Rome Tor Vergata (lower row) sites. The example reported here was performed considering the MODIS DB pixels within an area of radius 5 km around the site location and  $\Delta t_{max}$  (time between MODIS and AERONET observations) of  $\pm 30$  minutes. Both MODIS Aqua and Terra satellites are considered.

As made for the MODIS MAIAC AOD products, since MODIS DB AOD is retrieved at 470 nm, we exploited the AERONET AE between 440 and 870 nm to derive AERONET AOD at 470 nm using the same approach adopted in the previous section. In the inter-comparison shown in Fig. 6, we consider only MODIS DB AOD products that contain the AERONET site location (considering a 5 km maximum distance between the

center of the pixel and the site location) with  $\Delta t_{\max}$  between the MODIS satellite overpasses and AERONET observations of  $\pm 30$  minutes.

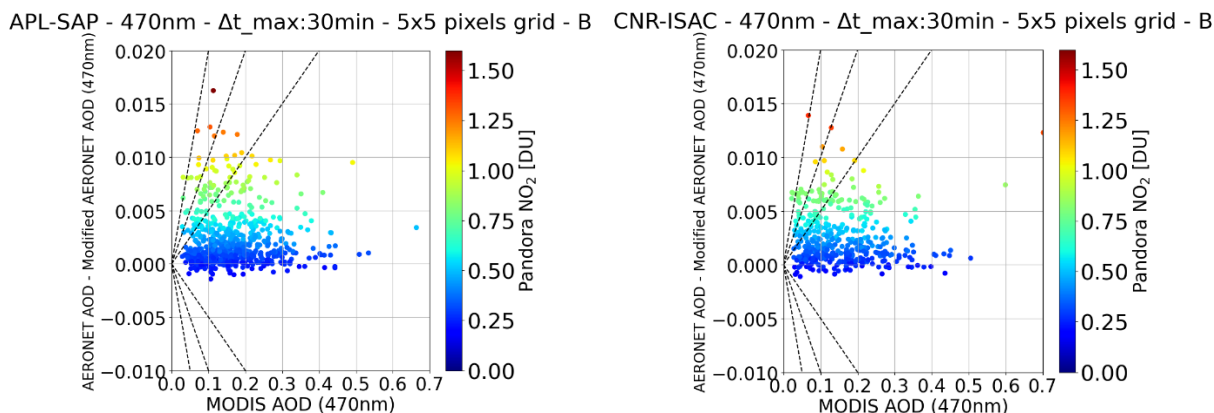


**Figure 7:** Analysis of the “improvement” computed as the AERONET AOD minus the “improved” AERONET AOD, as a function of MODIS DB AOD at 470 nm for Rome La Sapienza (upper row) and Rome Tor Vergata (lower row) sites. The example reported here was performed the MODIS DB pixels within an area of radius 5 km around the site location and  $\Delta t_{\max}$  (time between MODIS DB and AERONET observations) of  $\pm 30$  minutes.

In Fig. 7, we show the absolute correction as a function of the MODIS DB AOD and the NO<sub>2</sub> column retrieved by the Pandora instruments for both the Rome La Sapienza and Rome Tor Vergata sites. Although the improvement is, on average, relatively low (0.003), the correction can be larger than 10/20% in many cases (hotter colored dots). We can observe that the correction depends on the NO<sub>2</sub> amount by noting that the major “corrections” are represented by warmer colors, indicating high values of NO<sub>2</sub> retrieved by Pandora instruments.

To better evaluate the possible dependency of the agreement between MODIS DB and AERONET AOD products and the “improvement” from the period of the year, we computed the monthly averages of the different AOD datasets, the differences (MODIS DB minus AERONET) and the “improvement” for both sites (Fig. 8). This study is relative to a maximum distance between pixel centre and site location of 5 km and  $\pm 30$  minute as temporal criteria.



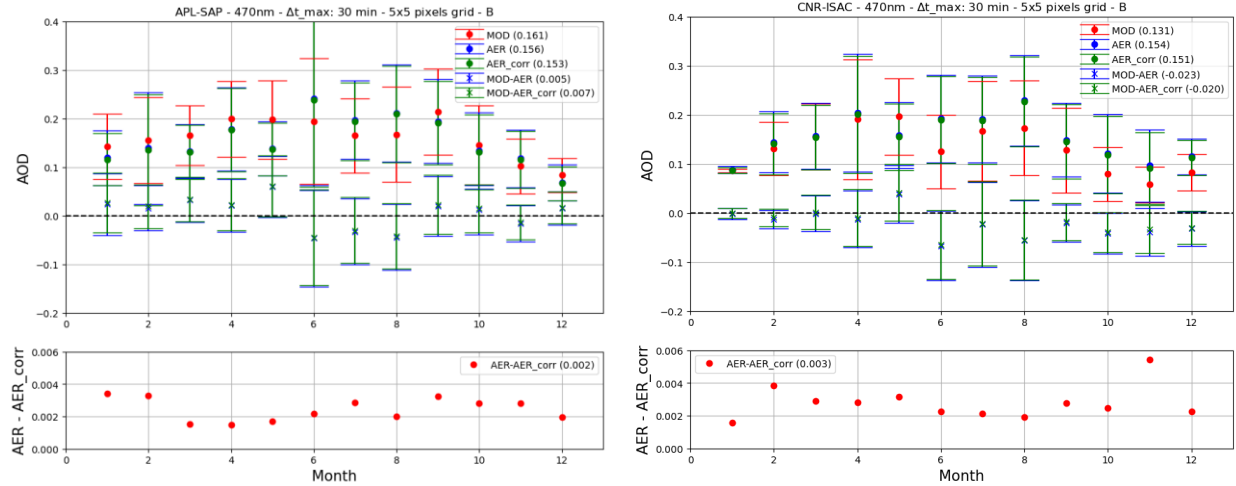


**Figure 8:** Analysis of the differences between MODIS DB and AERONET AOD at 470nm (upper panel of each plot) and of the “improvement” computed as the AERONET AOD minus the “improved” AERONET AOD, (lower panel of each plot) as a function of the month for Rome La Sapienza (upper plot) and Rome Tor Vergata (lower plot) sites. The example reported here was performed the MODIS DB pixels within an area of radius 5 km around the site location and  $\Delta t_{max}$  (time between MODIS DB and AERONET observations) of  $\pm 30$  minutes.

For both stations, Rome La Sapienza and Rome Tor Vergata, we generally observed a lower agreement between AERONET and MODIS DB AOD at 470 nm in the summer period (crosses in the upper panel of each plot). For Rome La Sapienza, the best agreement is in autumn/winter, where we observed a slightly positive bias (MODIS DB > AERONET). Instead, for Rome Tor Vergata, the agreement is better in the first months of the year. As observed during the analysis of MODIS MAIAC AOD products, the “improvement”, even if slight on average, goes in the right direction to cope with the differences between AERONET and MODIS DB AOD at 470 nm. The analysis does not highlight explicit dependency of the correction by the month.

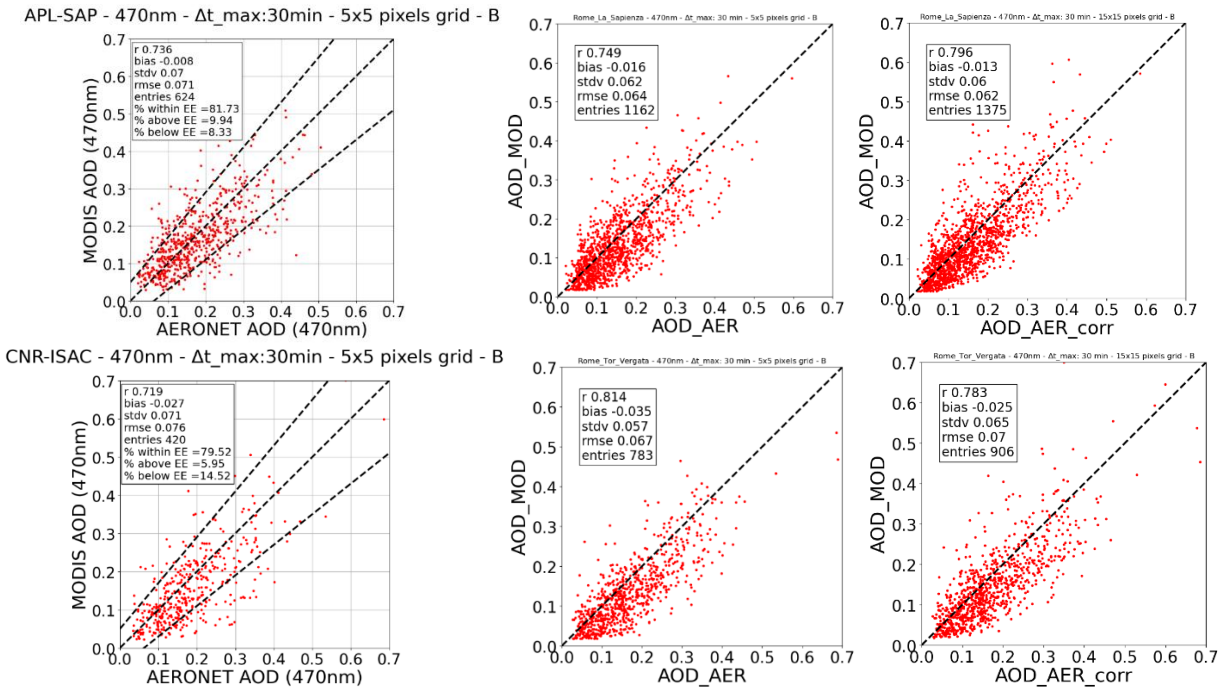


**Figure 9:** Comparison of the differences between MODIS DB and AERONET (first column, considering a maximum distance of 5 km between pixel center and site location), MODIS MAIAC and AERONET (second column, considering a 5x5 km grid centered on the site location), and MODIS MAIAC and AERONET (third column, considering a 15x15 km grid centered on the site location) AOD at 470 nm for Rome La Sapienza (upper row) and Rome Tor Vergata (lower row) sites. For all cases,  $\Delta t_{max}$  (time between MODIS DB and AERONET observations) is  $\pm 30$  minutes.

This exercise allowed us to evaluate the performances of two different MODIS AOD products against the AERONET AOD products for Rome La Sapienza and Rome Tor Vergata. In Fig. 9, we show the results of the inter-comparison between AERONET and MODIS DB and between AERONET and MODIS MAIAC AOD products. We fixed the time criteria  $\Delta t_{max}$  (time between MODIS satellite overpasses and AERONET observations) equal to  $\pm 30$  minutes. Regarding the spatial criteria, for MODIS DB, we considered the pixel (10 km of spatial resolution) that contains the site location adopting a  $\Delta d_{max}$  of 5 km (first column of Fig. 9). Instead, for MODIS MAIAC, we adopted two different spatial criteria: a regular grid of 5x5 and 15x15 km (second and third column of Fig. 9, respectively) around the pixel (1 km of spatial resolution) that contains the site location. Despite the lower spatial resolution, the MODIS DB AOD products show a better agreement against AERONET AOD for the Rome La Sapienza site. This result is expected because the MODIS DB algorithm exploits a pre-calculated land surface reflectance database in deep blue bands (0.412  $\mu\text{m}$ ) to enhance the quality of aerosol retrieval on bright surfaces. By contrast, for the Rome Tor Vergata site, we did not observe an improvement by using the MODIS DB because this site is a semi-rural location with darker surfaces around it with respect to the Rome La Sapienza site. This exercise highlights the variability of the characteristics of the area around Rome (the two sites' distance is about 13 km) and the complexity of the aerosol retrieval from satellite observations in such areas. In this context, super-sites such as Boundary-layer Air Quality-analysis Using Network of Instruments (BAQUININ) play an

essential role in this kind of Cal/Val activities. The results of the entire inter-comparison exercise obtained exploiting different co-location criteria are summarized in Tab. 2.

				MOD DB 470nm vs AER 470nm			MOD DB 470nm vs improved AER 470nm		
Site	$\Delta d_{max}$ (km)	$\Delta t_{max}$ (Minutes)	N	Bias (MOD DB - AER)	Std. Dev.	Corr	Bias (MOD DB - AER)	Std. Dev.	Corr
Rome La Sapienza	1	15	19	0.005	0.081	0.48	0.007	0.081	0.478
		30	19	0.004	0.081	0.484	0.006	0.081	0.482
		60	19	0.003	0.08	0.488	0.005	0.081	0.485
	5	15	612	-0.009	0.072	0.733	-0.007	0.072	0.736
		30	624	-0.008	0.07	0.736	-0.005	0.07	0.739
		60	639	-0.007	0.069	0.74	-0.005	0.068	0.744
	15	15	1316	-0.015	0.07	0.752	-0.013	0.069	0.755
		30	1349	-0.028	0.058	0.78	-0.024	0.057	0.779
		60	1368	-0.033	0.061	0.82	-0.029	0.06	0.822
Rome Tor Vergata	1	15	13	-0.014	0.083	0.173	-0.012	0.082	0.183
		30	13	-0.015	0.082	0.188	-0.013	0.081	0.197
		60	13	-0.017	0.081	0.204	-0.015	0.08	0.213
	5	15	392	-0.026	0.072	0.716	-0.023	0.072	0.717
		30	420	-0.027	0.071	0.719	-0.024	0.071	0.721
		60	437	-0.026	0.07	0.726	-0.024	0.07	0.728
	15	15	868	-0.027	0.07	0.738	-0.024	0.069	0.74
		30	931	-0.027	0.069	0.742	-0.024	0.068	0.744
		60	982	-0.036	0.066	0.777	-0.033	0.066	0.779

**Table 2:** Results of the analysis of the differences of MODIS DB (both Terra and Aqua) and AERONET AOD and MODIS DB and “improved” AERONET AOD at 470 nm for Rome La Sapienza and Rome Tor Vergata sites. The differences, the standard deviations and the correlations are reported as a function of the different spatio-temporal criteria adopted in the analysis: 1, 5 and 15 km for the spatial criteria, and  $\pm 15$ ,  $\pm 30$  and  $\pm 60$  minutes for the temporal criteria.

### 3.2.1 Extension of the inter-comparison against MODIS DB AOD data to other sites

The main results of the inter-comparison shown in Sect. 3.2 were included in [RD-7]. Adopting the same approach of [RD-7], 5 km for spatial criteria and  $\pm 30$  minutes for temporal criteria, we extended the inter-comparison against other sites where co-located AERONET and PGN instruments could provide AOD corrected at 440 nm. In the frame of WP2365, different areas were evaluated, and we focused on 3 of them: Dhaka, Mexico City and Beijing. The first two sites have been selected since we observed a significant difference between OMI NO<sub>2</sub> climatological values (used as input to the AERONET retrieval algorithm for the estimation of NO<sub>2</sub> spectral contribution at 440 nm) and PGN observations. On the other hand, the last site was selected because we observed that the PGN observations underestimate OMI

climatological values, contrary to what we observed in most of the analyzed sites. Table 3 summarizes the information on site location and the period considered for the analysis.

Name	Latitude (deg N)	Longitude (deg E)	Start Date (dd/mm/yyyy)	Stop Date (dd/mm/yyyy)	AERONET Level
DHAKA	23.72839	90.39819	01/01/2023	06/06/2023	1.5
MEXICO CITY	19.33361	-99.18167	27/10/2019	07/12/2021	1.5
BEIJING	39.97689	116.38137	30/07/2021	16/06/2023	1.5

**Table 3:** Information on the three sites included in the extension of the inter-comparison against MODIS DB AOD products.

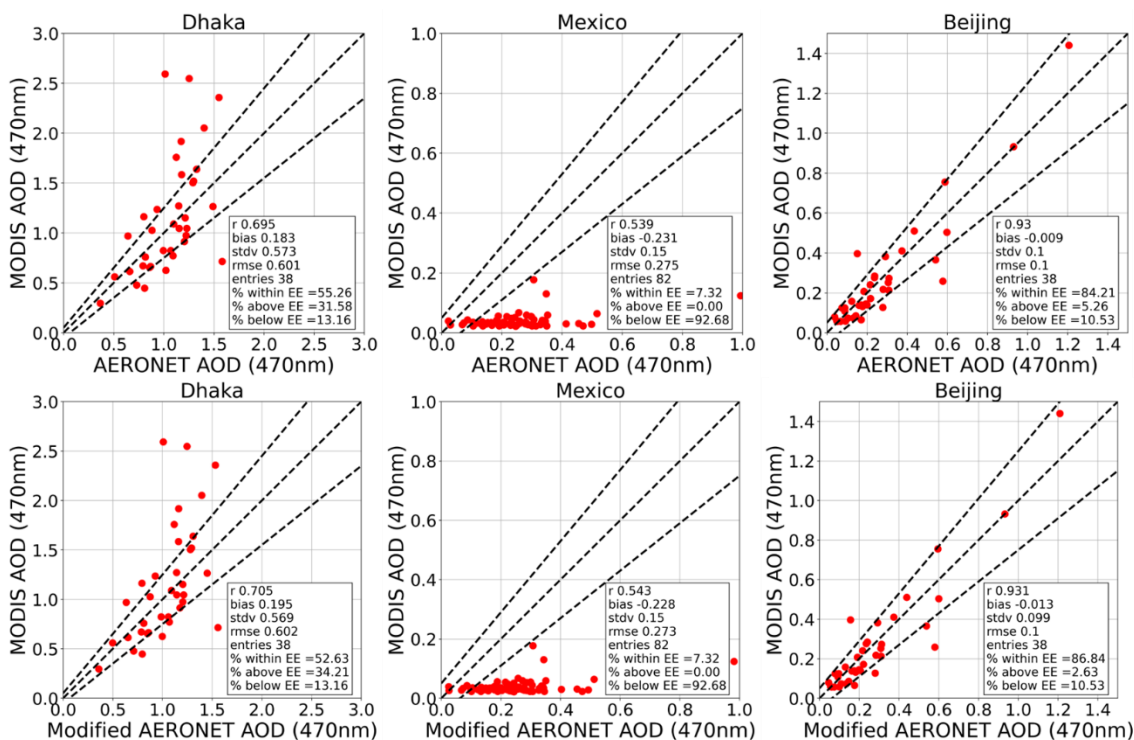


**Figure 10:** Inter-comparison of MODIS DB and AERONET AOD (upper row) and MODIS DB and “Modified” AERONET (lower row) AOD at 470nm for Dhaka (first column), Mexico City (second column) and Beijing (third column) sites. The example reported here was performed considering the MODIS DB pixel that contains the site location and  $\Delta t_{max}$  (time between MODIS and AERONET observations) of  $\pm 30$  minutes. Both MODIS Aqua and Terra satellites are considered.

In Fig. 10, we observe that for the Mexico City case, as reported in [RD-8], the MODIS DB data availability is quite low and, for the available pixels, the AOD values are very low, which is inconsistent with the AERONET measurements. This behavior is quite typical of sites located at very high altitudes (> 2000 m), such as Mexico City (2.240 m). Nevertheless, after the application of the correction, we observed a slight improvement (in terms of bias) in the agreement of the AERONET AOD products against MODIS DB ones.

Instead, the correction goes the wrong way in the Dhaka and Beijing cases, reducing the agreement against the MODIS DB AOD products. It is important to note that the limited number of matchups could affect the quality of the assessment. For Dhaka analysis, this reduced number of matchups is because of the limited period we analyzed. Instead, for the Beijing case, we have a reduced number of matchups mainly due to the poor quality of Pandora data since most of them are flagged as "unusable high/medium/low quality".

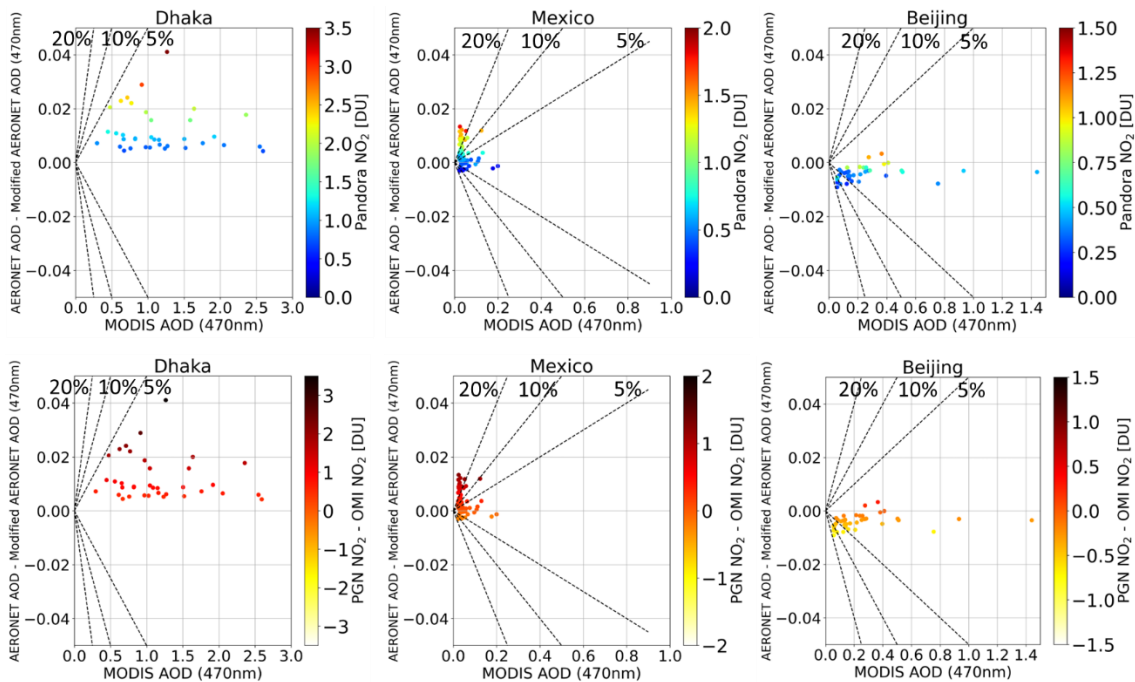


**Figure 11:** Analysis of the “improvement” computed as the AERONET AOD minus the “improved” AERONET AOD, as a function of MODIS DB AOD at 470 nm for for Dhaka (first column), Mexico City (second column) and Beijing (third column) sites. The example reported here was performed the MODIS pixel that contains the site location and  $\Delta t_{max}$  (time between MODIS DB and AERONET observations) of  $\pm 30$  minutes. The coloured scales report the Pandora NO<sub>2</sub> column (upper row) and the difference between the Pandora NO<sub>2</sub> column and the OMI NO<sub>2</sub> column (lower row) for each matchup.

In Fig. 11, we show the absolute correction as a function of the MODIS DB AOD and the NO<sub>2</sub> column retrieved by the Pandora instruments (upper row) and the difference between the Pandora NO<sub>2</sub> column and the OMI NO<sub>2</sub> column (lower row) for the three different sites. As already highlighted, the correction

only depends on the NO<sub>2</sub> amount and not on the AOD. Figure 11 also highlights that the improvement is, on average, higher for Dhaka (0.012) and lower for Mexico City and Beijing (-0.013 and 0.004, respectively). In general, as observed for Rome La Sapienza and Rome Tor Vergata sites, although the improvement is on average relatively low, the correction can be larger than 10/20% in many cases.

### 3.3 Inter-comparison of AERONET AOD products against S-3 SYN AOD data

For the S-3 SYN AOD products, the AOD at 440 nm is computed on the so-called super-pixels, an 11 by 11 pixels grid (4.5 x 4.5 km considering the OLCI spatial resolution of 300 m) centered on the pixel containing the in-situ station. Since the S-3 SYN AOD products are provided separately for S-3A and S-3B satellites and considering whether the SLSTR single or dual view is exploited during the AOD retrieval, we analyzed the impact of these two factors on the agreement. About the AERONET AOD at 440 nm products, we consider all original AERONET products and the “improved” ones within a time window of  $\pm 30$  minutes from the satellite overpass time. As spatial criteria, we consider an area within a radius of 10 km and 25 km from the site’s location (Figures 13a and 13b). The 25 km spatial criteria slightly follows the approach adopted in [RD-9], where a surface of ca. 50 km x 50 km around each station is considered for the matchup identification. In Fig. 12, we report the results of the analysis for S-3 SYN products computed exploiting the S-3A SLSTR dual view observations. The results of the complete analysis are reported in Table 4a and 4b, considering respectively 10 km and 25 km of maximum distance between the center of the S-3 SYN AOD pixel and site location.

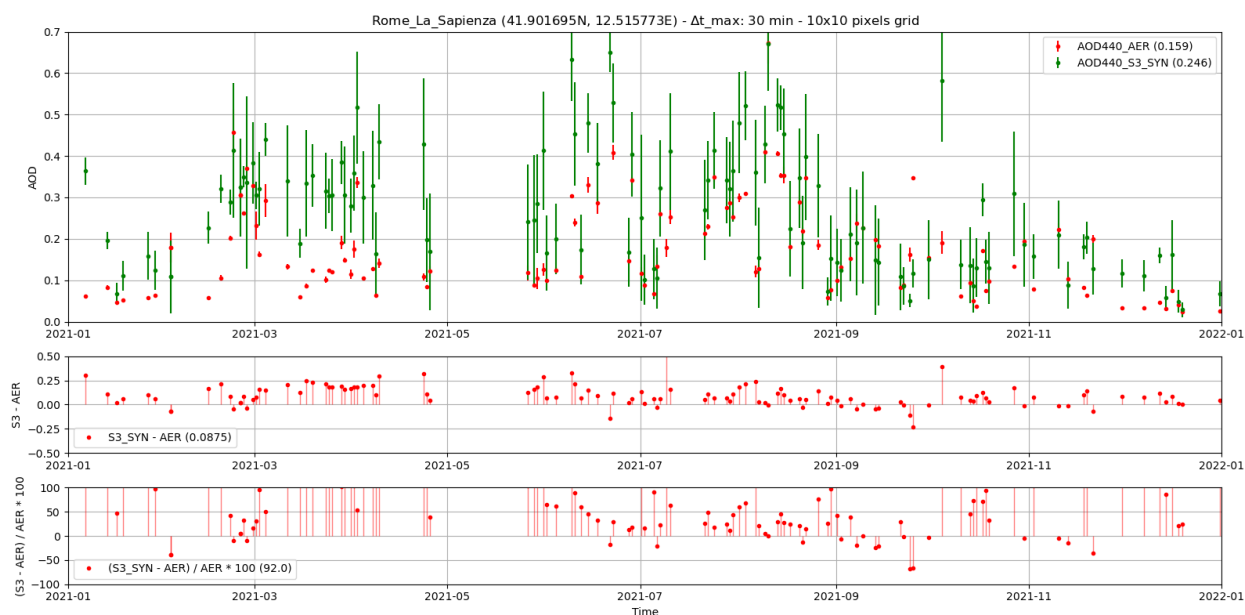


**Figure 12:** Analysis of S-3 SYN, AERONET and “improved” AERONET AOD at 440 nm products (upper panel), and corresponding absolute (middle panel) and percentage (lower panel) differences for Rome La Sapienza AERONET site. In this example, S-3 SYN products are computed exploiting the S-3A SLSTR dual view observations.

				S3 SYN AOD 440nm vs AER AOD440nm			S3 SYN AOD 440nm vs AER AOD440nm corrected		
Site	S3	View	N	Bias (S3-AER)	Std. Dev.	Corr.	Bias (S3-AER)	Std. Dev.	Corr.
Rome La Sapienza	A	Single	26	0.252	0.144	0.788	0.254	0.144	0.789
		Dual	151	0.095	0.099	0.681	0.097	0.099	0.681
	B	Single	33	0.204	0.106	0.813	0.206	0.105	0.821
		Dual	250	0.079	0.095	0.678	0.082	0.095	0.677
Rome Tor Vergata	A	Single	31	0.151	0.123	0.37	0.156	0.122	0.383
		Dual	58	0.053	0.104	0.502	0.057	0.105	0.499
	B	Single	57	0.128	0.132	0.421	0.133	0.132	0.419
		Dual	114	0.045	0.093	0.537	0.048	0.093	0.533

**Table 4a:** Summary of the results of the inter-comparison S-3 SYN and AERONET, “improved” and not, AOD products at 440 nm, considering the S-3 SYN pixel that contains the site location with  $\Delta d_{max}$  of 10 km and  $\Delta t_{max}$  (time between S-3 SYN and AERONET observations) of  $\pm 30$  minutes.

				S3 SYN AOD 440nm vs AER AOD440nm			S3 SYN AOD 440nm vs AER AOD440nm corrected		
Site	S3	View	N	Bias (S3-AER)	Std. Dev.	Corr.	Bias (S3-AER)	Std. Dev.	Corr.
Rome La Sapienza	A	Single	121	0.178	0.149	0.687	0.181	0.149	0.69
		Dual	179	0.066	0.113	0.666	0.068	0.113	0.668
	B	Single	204	0.148	0.315	0.493	0.151	0.315	0.496
		Dual	292	0.054	0.102	0.694	0.056	0.101	0.695
Rome Tor Vergata	A	Single	51	0.19	0.137	0.535	0.194	0.136	0.548
		Dual	63	0.064	0.101	0.509	0.068	0.101	0.508
	B	Single	98	0.165	0.141	0.495	0.169	0.14	0.501
		Dual	126	0.059	0.093	0.518	0.063	0.093	0.516

**Table 4b:** Summary of the results of the inter-comparison S-3 SYN and AERONET, “improved” and not, AOD products at 440 nm, considering the S-3 SYN pixel that contains the site location with  $\Delta d_{max}$  of 25 km and  $\Delta t_{max}$  (time between S-3 SYN and AERONET observations) of  $\pm 30$  minutes.

The inter-comparison between S-3 SYN and AERONET, “improved” and not, AOD products at 440 nm highlighted as the S-3 SYN products generally overestimate AERONET products. We observed a better agreement considering S-3 SYN AOD products retrieved by exploiting the SLSTR dual view. This result is expected considering that retrievals exploiting SLSTR dual view give higher quality by making use of more information to allow less reliance on surface spectral assumptions. Evaluating the performances of one

satellite against the other one, S-3B works slightly better considering both configurations, single and dual-view. Focusing on the time series, as in Fig. 12, we observed that the agreement improves in the summer period, even showing matchups where the differences are negative (S-3 SYN AOD < AERONET AOD). As already observed in the previous sections, the agreement between S3\_SYN and AER AOD slightly (0.002/0.003) decreases after the correction to the AERONET AOD is applied (Table 4a and 4b).

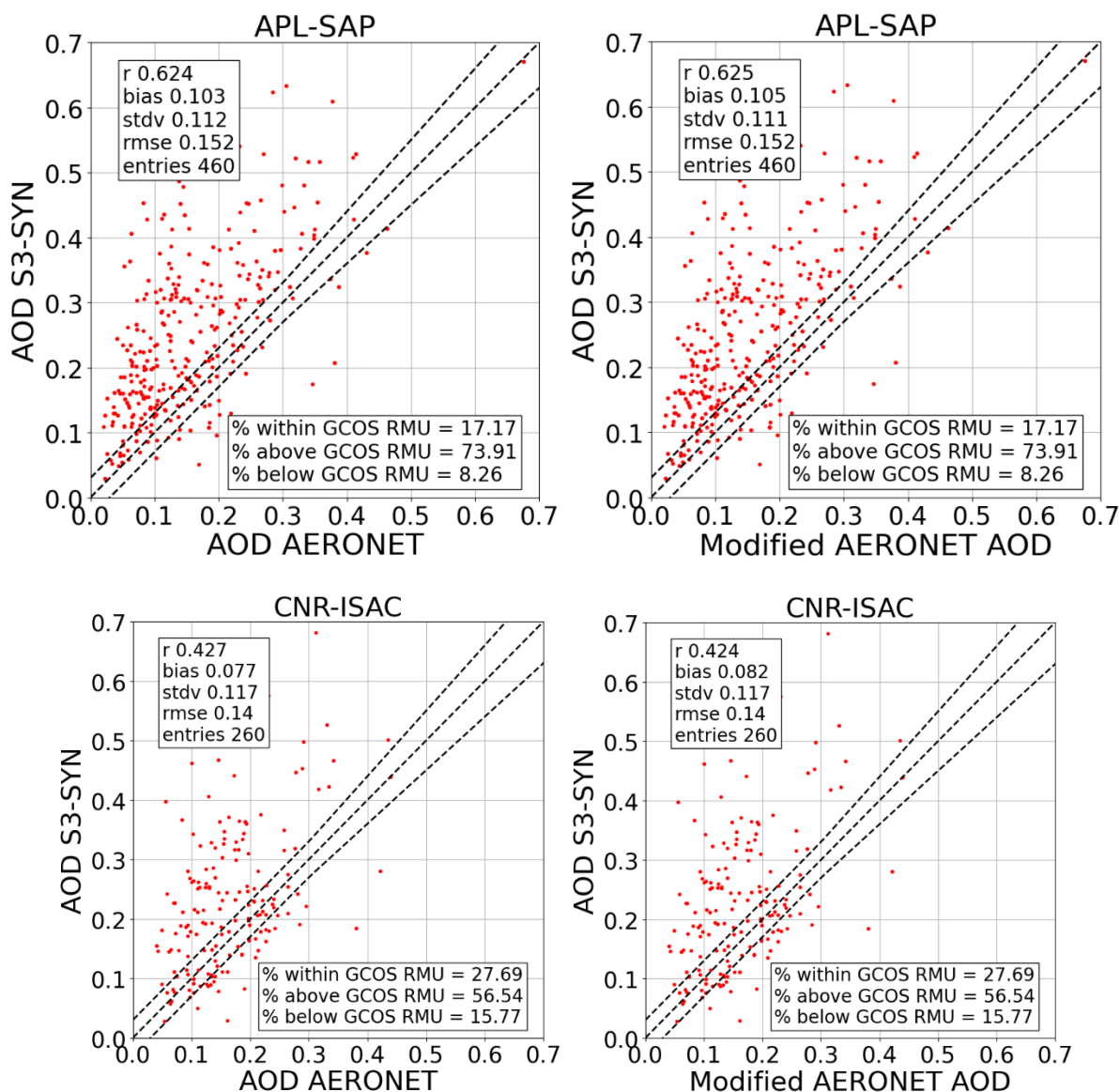


**Figure 13 a:** Inter-comparison of S-3 SYN and AERONET AOD (left column) and S-3 SYN and “modified” AERONET (right column) AOD at 470nm for Rome La Sapienza (upper row) and Rome Tor Vergata (lower row) sites. The example reported here was performed considering the S-3 SYN pixel that contains the site location with  $\Delta d_{max}$  of 10 km and  $\Delta t_{max}$  (time between S-3 SYN and AERONET observations) of  $\pm 30$  minutes.



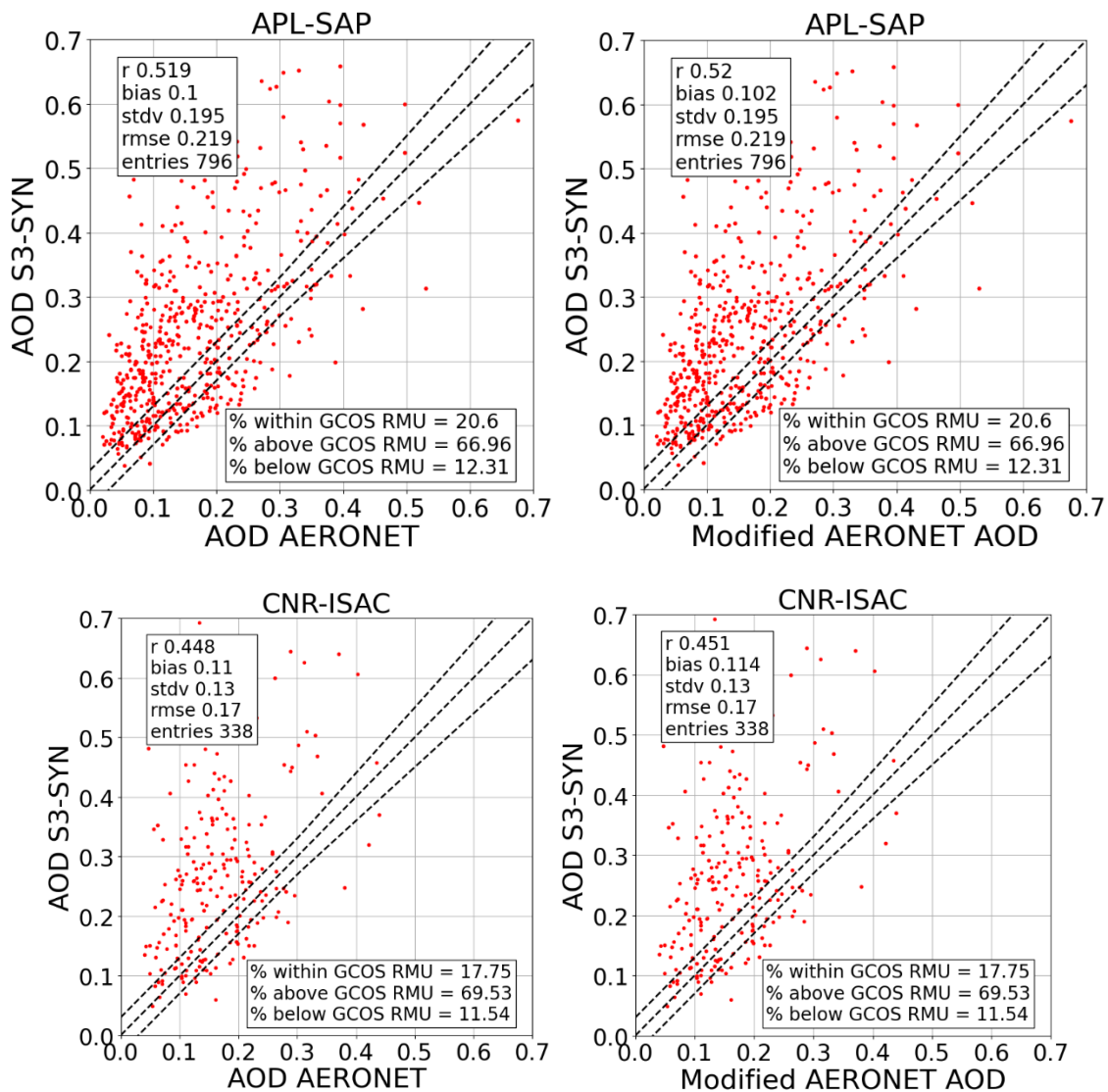
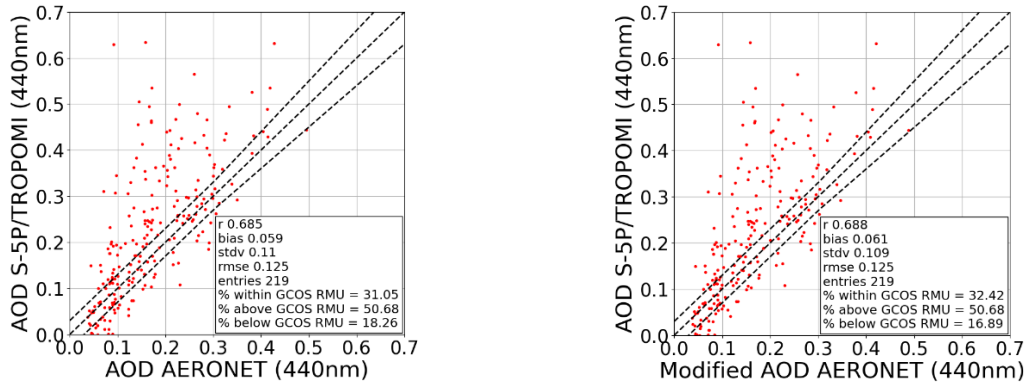


**Figure 13 b:** Inter-comparison of S-3 SYN and AERONET AOD (left column) and S-3 SYN and “Modified” AERONET (right column) AOD at 470nm for Rome La Sapienza (upper row) and Rome Tor Vergata (lower row) sites. The example reported here was performed considering the S-3 SYN pixel that contains the site location with  $\Delta d_{max}$  of 25 km and  $\Delta t_{max}$  (time between S-3 SYN and AERONET observations) of  $\pm 30$  minutes.

### 3.4 Inter-comparison of AERONET AOD products against S-5P+ AOD data

We started the inter-comparison between AERONET and S-5P+ AOD products considering as co-location criteria a maximum distance of 5 km between the center of TROPOMI pixel and the site location and a  $\Delta t_{max}$ , the time between S-5P+ and AERONET observations, of  $\pm 30$  minutes (Fig. 14). We also observe that the differences between S-5P+ and AERONET AOD products are on average similar (Fig. 14 and Tab. 5) between the Rome Tor Vergata site and Rome La Sapienza site, 0.055 and 0.059, respectively. The correlation between the two datasets is slightly higher for the Rome La Sapienza AERONET site. The applied correction, as already seen for S-3 SYN AOD products, introduces a slight increase of the bias of about 0.002/0.003.

APL-SAP - 440nm -  $\Delta t_{max}$ :30min - 5x5 pixels grid - B APL-SAP - 440nm -  $\Delta t_{max}$ :30min - 5x5 pixels grid - B



CNR-ISAC - 440nm -  $\Delta t_{max}$ :30min - 5x5 pixels grid - B CNR-ISAC - 440nm -  $\Delta t_{max}$ :30min - 5x5 pixels grid - B

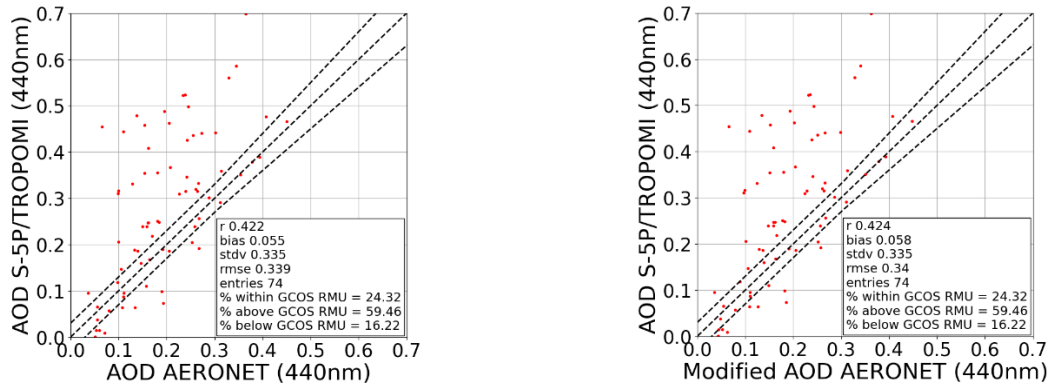


**Figure 14:** Inter-comparison of S-5P+ and AERONET AOD (left column) and S-5P+ and “improved” AERONET (right column) AOD at 440 nm for Rome La Sapienza (upper row) and Rome Tor Vergata (lower row) sites. The example reported here was performed considering a maximum distance of 5 km between the center of TROPOMI pixel and the site location and  $\Delta t_{max}$  (time between S-5P+ and AERONET observations) of  $\pm 30$  minutes.

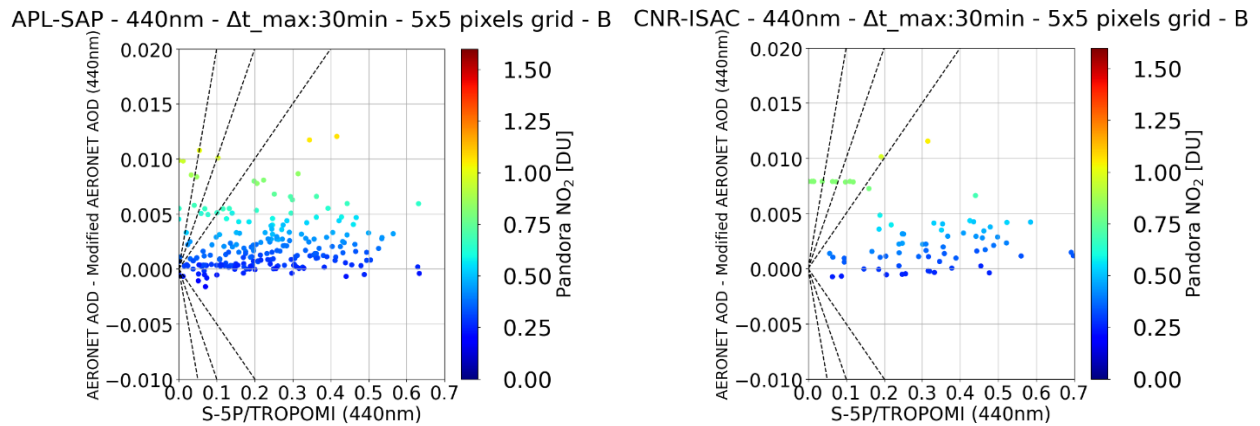


**Figure 15:** Analysis of the “improvement” computed as the AERONET AOD minus the “improved” AERONET AOD, as a function of S-5P+ AOD at 440 nm for Rome La Sapienza (upper row) and Rome Tor Vergata (lower row) sites. The example reported here was performed a maximum distance of 5 km between the center of TROPOMI pixel and the site location and  $\Delta t_{max}$  (time between S-5P+ and AERONET observations) of  $\pm 30$  minutes.

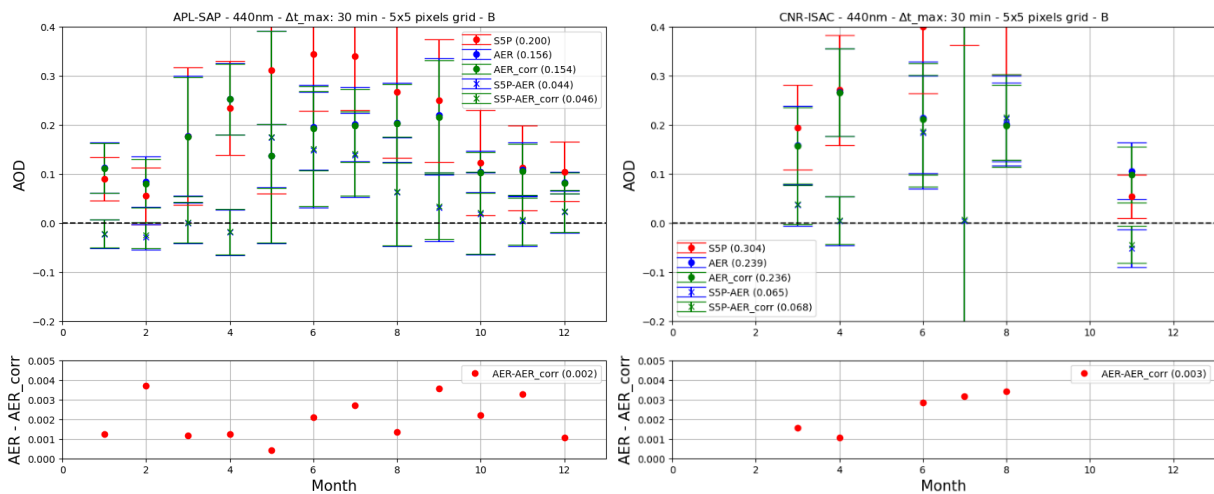


**Figure 16:** Analysis of the differences between S-5P+ and AERONET AOD at 440 nm (upper panel of each plot) and of the “improvement” computed as the AERONET AOD minus the “improved” AERONET AOD, (lower panel of each plot) as a function of the month for Rome La Sapienza (upper plot) and Rome Tor Vergata (lower plot) sites. The example reported here was performed considering a maximum distance of 5 km between the center of TROPOMI pixel and the site location and  $\Delta t_{max}$  (time between S-5P+ and AERONET observations) of  $\pm 30$  minutes.

To evaluate the possible dependency of the agreement between S-5P+ and AERONET AOD products and the “improvement” from the different periods of the year, we computed the monthly averages of the different AOD datasets, the differences (S-5P+ minus AERONET) and the “improvement” for both sites (Fig. 16).

In this analysis, focusing on Rome La Sapienza results that properly cover the entire period, we observed a lower agreement between AERONET and S-5P+ in the summer period (Figure 16, upper graphs). The agreement improves during autumn and winter, and some months show slightly negative bias (AERONET > S-5P+). The introduced “correction” is higher during Summer and Autumn, even if it does not show a clear dependency by the season.

As highlighted before, considering the distance between the two sites and the temporal variability of aerosol distribution, this co-location criteria represents the most meaningful criteria from a physical point of view. As already done before, we performed the same analysis even considering different criteria: 15 km for the spatial criteria and  $\pm 15$ ,  $\pm 30$  and  $\pm 60$  minutes for the temporal criteria. The results of the analysis are reported in the following Table 5. To improve the readability of the results, we also summarize in Figure 17 the analysis of the differences (S-5P+ minus AERONET AOD at 440 nm) as a function of the co-location criteria for AERONET sites.

				S5P 440nm vs AER 440nm			S5P 440nm vs improved AER 440nm		
Site	$\Delta d_{max}$	$\Delta t_{max}$	N	Bias (S5P- AER)	Std. Dev.	Corr.	Bias (S5P- AER)	Std. Dev.	Corr.
Rome La Sapienza	5 km	15	213	0.058	0.11	0.672	0.06	0.11	0.676
		30	219	0.059	0.11	0.685	0.061	0.109	0.688
		60	223	0.058	0.11	0.68	0.06	0.11	0.683
	15 km	15	267	0.123	0.131	0.65	0.125	0.131	0.653
		30	277	0.125	0.13	0.656	0.127	0.13	0.66
		60	286	0.126	0.131	0.651	0.128	0.131	0.654
Rome Tor Vergata	5 km	15	65	0.046	0.354	0.432	0.049	0.354	0.434
		30	74	0.055	0.335	0.422	0.058	0.335	0.424
		60	85	0.059	0.316	0.413	0.062	0.316	0.414
	15 km	15	77	0.054	0.335	0.378	0.057	0.335	0.38
		30	94	0.062	0.307	0.371	0.065	0.307	0.373
		60	109	0.066	0.291	0.352	0.069	0.291	0.354

**Table 5:** Results of the analysis of the differences of S-5P+ and AERONET AOD and S-5P+ and “improved” AERONET AOD at 440 nm for Rome La Sapienza and Rome Tor Vergata sites. The differences, the standard deviations and the correlations are reported as a function of the different spatio-temporal criteria adopted in the analysis: 5 and 15 km for the spatial criteria, and  $\pm 15$ ,  $\pm 30$  and  $\pm 60$  minutes for the temporal criteria.

We observe that the difference between S-5P+ and AER and the standard deviation increase as the area's dimension increases, which is more evident for Rome La Sapienza. We also note that the agreement between S-5P+ and AERONET AOD slightly decreases (0.002 for Rome La Sapienza and 0.003 for Rome Tor Vergata) after applying the correction to the AERONET AOD, despite the improvement of the other statistics (the correlation increases and the standard deviation decreases).

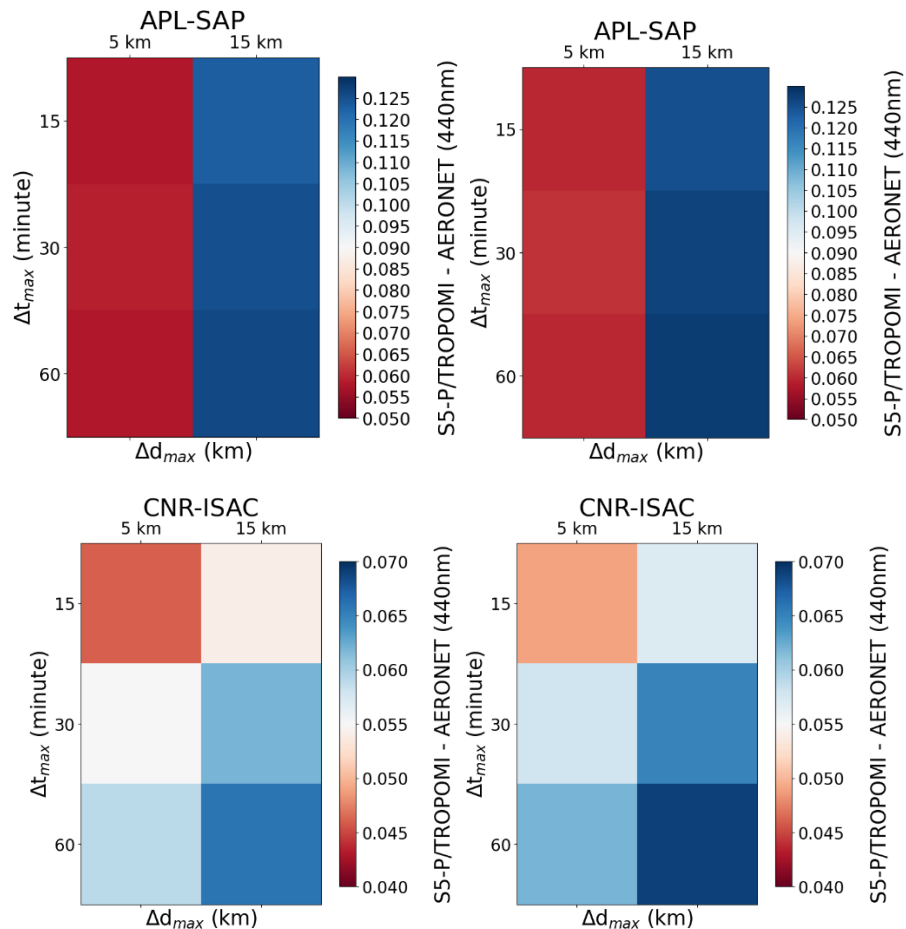


**Figure 17:** Analysis of the differences of S-5P+ and AERONET AOD (left column) and S-5P+ and “improved” AERONET (right column) AOD at 440nm for Rome La Sapienza (upper row) and Rome Tor Vergata (lower row) sites. The differences in each plot are reported as a function of the different spatio-temporal criteria adopted in the analysis: 5x5 and 15x15 km for the spatial criteria, and  $\pm 15$ ,  $\pm 30$  and  $\pm 60$  minutes for the temporal criteria.

## 4 Conclusions

To assess the quality of the AERONET AOD products, we performed an inter-comparison of these products and corrected ones against four satellite AOD products: the MODIS MAIAC, the MODIS DB, the S3 SYNERGY, and the S-5P+/TROPOMI AOD products. This comparison was carried out by choosing different sets of criteria. For MODIS MAIAC, since the products are provided on a 1 km x 1 km regular grid, we worked with grids of 1x1 km, 5x5 km and 15x15 km as spatial criteria, and  $\pm 15$ ,  $\pm 30$  and  $\pm 60$  minutes of offset between the ground and the satellite AOD products as temporal criteria. For MODIS DB AOD products, as spatial criteria, we considered the distance between the center of the pixel and site location by adopting 1, 5, and 15 km of maximum distance. The same approach was adopted with S5P+. S3 SYN AOD products were studied considering 10 and 25 km of maximum distance and a time interval of  $\pm 30$  minutes. For these last products, the performances of the different view modes and the different satellites were assessed.

We started performing the inter-comparison between MODIS MAIAC and AERONET AOD products at 470 nm for Rome La Sapienza and Rome Tor Vergata AERONET sites. We tested several co-location criteria observing that MODIS MAIAC generally underestimate AERONET AOD products. Considering a 5x5 km grid centered at the site location and  $\Delta t_{\max}$  (time between MODIS MAIAC and AERONET observations) of  $\pm 30$  minutes as co-location criteria, we observed a bias (MODIS MAIAC minus AERONET) of -0.016 for Rome La Sapienza and -0.035 for Rome Tor Vergata. The correlation is high for both sites, higher for Rome Tor Vergata (0.814) than for Rome La Sapienza (0.749). We generally observed a lower agreement between AERONET and MODIS MAIAC AOD at 470 nm in the summer period for both stations. The “improvement” in the existing AERONET AOD products induced by the correction exploiting the Pandora NO<sub>2</sub> VCDs (see [RD-1] for more details) introduces a slight improvement (0.002/0.003) in the agreement between MODIS MAIAC and AERONET AOD products. Even if we did not observe evident dependency of the “improvement” by the AOD absolute value, we observed that some “improvements” are 15/20%. To better understand possible effects induced by the fact that MODIS MAIAC uses an AERONET-based climatology (static and does not account for seasonal variations of the aerosol properties) in the computation of AOD products, we will perform a further inter-comparison against the MODIS Collection 6.1 data that provides the updated DB AOD products [RD-4].

The MODIS DB algorithm was originally developed to retrieve AOD over bright surfaces with 10 km spatial resolution, utilizing the 0.412 and 0.47/0.65  $\mu\text{m}$  wavelengths depending on the surface type. The new Collection 6.1 DB algorithm extends retrievals to green and dark surfaces and provides global AOD except over snow and ice. As made for the MODIS MAIAC AOD products, we compared MODIS DB AOD and AERONET AOD data at 470 nm. We performed the inter-comparison considering MODIS DB AOD products within circles of radius 1, 5 and 15 km around the AERONET site location and the AERONET AOD data with  $\Delta t_{\max}$  between the MODIS satellite overpasses and AERONET observations of  $\pm 30$  minutes. Considering the 5 km maximum distance, we noted that, even if the correlation between the two datasets is almost similar for the two sites, the differences between MODIS DB and AERONET AOD products are 3/4 times (-0.027 against -0.008) larger for the Rome Tor Vergata site with respect to the Rome La Sapienza site. Even if slight on average (0.002), the “improvement” goes in the right direction to cope with the differences between AERONET and MODIS DB AOD at 470 nm. This happens for every analysed scenario but for the one considering Rome La Sapienza site with a grid of 1x1km as special criteria: in this case only, MODIS

DB overestimates AERONET, and the correction goes in the wrong direction, being the bias positive and greater for the corrected AOD values. Despite the relative low improvement (on average), we observed as it is higher than 10/15% in some cases. The best agreement is in the autumn/winter period, where we observed a slightly positive bias (AERONET < MODIS DB). We preliminarily evaluate the different performances of MODIS DB and MODIS MAIAC AOD products against the AERONET AOD products of Rome La Sapienza and Rome Tor Vergata. We observed that the MODIS DB AOD products show a better agreement against AERONET AOD for the Rome La Sapienza site. This result is expected since the MODIS DB algorithm approach for the retrieval of aerosol on bright surfaces. On the other hand, we did not observe a comparable improvement by using the MODIS DB for the Rome Tor Vergata site. This result is probably because this site is a semi-rural location with darker surfaces around with respect to the Rome La Sapienza site, and it does not benefit from the DB approach. More generally, this simple inter-comparison highlights the complexity and variability of the characteristic of the area around Rome and the difficulties that we have to face for aerosol retrieval from satellite observations in such areas. On this point, it is important to stress the essential role that super-sites such as BAQUININ play in this kind of Cal/Val activity.

The main results of the inter-comparison against MODIS DB were included in [RD-7]. Adopting the same approach of the paper, we extended the inter-comparison to other sites (Dhaka, Mexico City and Beijing). For the Mexico City case, despite MODIS DB data availability was quite low and the AOD values are very low due to very high altitudes of Mexico City (2.240 m), after the application of the correction, we observed an improvement in the agreement of the AERONET AOD products against MODIS DB ones. The correction goes the wrong way in the Dhaka and Beijing cases, reducing the agreement against the MODIS DB AOD products. In these cases, the limited number of matchups could affect the quality of the assessment. For Dhaka analysis, this reduced number of matchups is because of the limited period we analyzed. Instead, for the Beijing case, we have a reduced number of matchups mainly due to the poor quality of Pandora data considering that most of them are flagged as "unusable high/medium/low quality". More generally, the improvement is, on average, higher for Dhaka (0.012) and lower for Mexico City and Beijing (-0.013 and 0.004, respectively). As already observed for the Rome La Sapienza and Rome Tor Vergata sites, although the improvement is relatively slight on average, the correction can be larger than 10/20% in many cases.

The AERONET AOD products at 440 nm have also been compared with the S-3 SYN AOD products, exploiting the coincidences for both Rome La Sapienza and Rome Tor Vergata AERONET sites for 2020-2022. The inter-comparison between S-3 SYN and AERONET highlights that S-3 SYN AOD products generally overestimate AERONET products, with a better agreement considering S-3 products retrieved exploiting the SLSTR dual view. At the same time, the performances of S-3B satellite against S-3a show a better agreement. Contrary to what we observed for MODIS MAIAC, the agreement improved in the summer period. The agreement between S-3 SYN and AERONET AOD products slightly (0.002/0.003) decreases after applying the correction to the AERONET AOD.

At the same time, to better evaluate the effects of the improvement of the AERONET AOD products and increase our knowledge of very recently developed AOD products, we will extend our exercise by including an inter-comparison against the new ESA S-5P+ Innovation AOD/BRDF products (<https://eo4society.esa.int/projects/sentinel-5p-innovation-aod-brdf/>). The project's main objective was to characterize aerosol properties from S-5P TROPOMI measurements by developing an algorithm capable of providing AOD and information about the absorption and type of the aerosol. One key element of the

approach employed in the project was using the GRASP as a state-of-the-art retrieval strategy for generating enhanced aerosol and BRDF products from Sentinel-5p. We started the inter-comparison between AERONET and S-5P+ AOD products for the 2019-2020 period considering as co-location criteria a maximum distance of 5 km between the center of TROPOMI pixel and the site location and a  $\Delta t_{max}$ , the time between S-5P+ and AERONET observations, of  $\pm 30$  minutes. S-5P+ AOD products generally overestimate AERONET products for both sites. We also observe that the differences between S-5P+ and AERONET AOD products are more significant (about 2 times larger) for the Rome La Sapienza site with 15x15km grid (0.12) against all other cases (0.06). The bias for the two datasets is on average about 0.09 for Rome La Sapienza and 0.06 for Rome Tor Vergata. Despite what was observed in the inter-comparison with the other satellite borne AOD products, we did not observe a relation between the period of the year and the agreement between those products. As observed in the inter-comparison against S-3 SYN AOD products, the correction decreases the agreement by about 0.002 on average. As done before, we tested different criteria: 5 and 15 km for the spatial criteria and  $\pm 15$ ,  $\pm 30$  and  $\pm 60$  minutes for the temporal criteria. We noted that the difference between S-5P+ and AER and the standard deviation increase as the area's dimension increases, which is more evident for Rome La Sapienza.